



Automatic bronchial segmentation on ultra-HRCT scans: advantage of the 1024-matrix size with 0.25-mm slice thickness reconstruction

Yuka Morita¹ · Tsuneo Yamashiro¹ · Nanae Tsuchiya¹ · Maho Tsubakimoto¹ · Sadayuki Murayama¹

Received: 18 March 2020 / Accepted: 5 June 2020 / Published online: 19 June 2020
© Japan Radiological Society 2020

Abstract

Purpose The aim of this study was to evaluate the advantages of ultra-high-resolution computed tomography (U-HRCT) for automatic bronchial segmentation.

Materials and methods This retrospective study was approved by the Institutional Review Board, and written informed consent was waived. Thirty-three consecutive patients who underwent chest CT by a U-HRCT scanner were enrolled. In each patient, CT data were reconstructed by two different protocols: 512×512 matrix with 0.5-mm slice thickness (conventional HRCT mode) and 1024×1024 matrix with 0.25-mm slice thickness (U-HRCT mode). We used a research workstation to compare the two CT modes with regard to the numbers and total lengths of the automatically segmented bronchi.

Results Significantly greater numbers and longer lengths of peripheral bronchi were segmented in the U-HRCT mode than in the conventional HRCT mode ($P < 0.001$, for fifth- to eighth-generation bronchi). For example, the mean numbers and total lengths of the sixth-generation bronchi were 81 and 1048 mm in the U-HRCT mode and 59 and 538 mm in the conventional HRCT mode.

Conclusions The U-HRCT mode greatly improves automatic airway segmentation for the more peripheral bronchi, compared with the conventional HRCT mode. This advantage can be applied to routine clinical care, such as virtual bronchoscopy and automatic lung segmentation.

Keywords Ultra-high-resolution computed tomography · Bronchus · Airway segmentation · Quantitative measurement

Electronic supplementary material The online version of this article (<https://doi.org/10.1007/s11604-020-01000-9>) contains supplementary material, which is available to authorized users.

✉ Yuka Morita
yukamorita.02feb@gmail.com

Tsuneo Yamashiro
clatsune@yahoo.co.jp

Nanae Tsuchiya
ntsuchi@med.u-ryukyu.ac.jp

Maho Tsubakimoto
tsubaki@med.u-ryukyu.ac.jp

Sadayuki Murayama
sadayuki@med.u-ryukyu.ac.jp

¹ Department of Radiology, Graduate School of Medical Science, University of the Ryukyus, 207 Uehara, Nishihara, Okinawa 903-0215, Japan

Introduction

Automatic airway segmentation by pulmonary computed tomography (CT) is a basic technique for obtaining various quantitative measurements of the airways and lungs. For example, CT-based quantitative evaluation of bronchi has been increasingly investigated. In patients with chronic obstructive pulmonary disease (COPD), CT airway indices such as luminal area, percentage of airway wall area, and peak wall attenuation have been shown to be correlated with several spirometric parameters such as forced expiratory volume in 1 s [1–3]. The correlation was notably stronger for the peripheral airways than for the proximal airways.

Histopathological examinations of human lungs have indicated that peripheral bronchi with internal diameters < 2 mm are the major determinant of airflow limitation in obstructive lung diseases [4]. Although several studies have reported that conventional high-resolution CT (HRCT) can be used to assess wall thickening and luminal narrowing of different bronchial generations [1–3], because of

limitations in the spatial resolution of conventional HRCT, these investigations so far have not been able to address the more peripheral airways such as the sixth, seventh, and eighth bronchial generations. Thus, for these peripheral bronchi, improved automatic airway segmentation is needed to obtain more reliable information on CT airway indices in COPD and other obstructive diseases.

Recent advances in CT technology have led to ultra-HRCT (U-HRCT), which can provide CT images with a 1024×1024 matrix and 0.25-mm slice thickness reconstruction. The advantages in image quality provided by U-HRCT have been reported for various imaging fields such as CT angiography and chest CT [5–13]. For example, it has been reported that the artery of Adamkiewicz is better depicted on U-HRCT scans with 0.25-mm thickness than on regular HRCT scans with 0.5-mm thickness [9]. It has also been shown that CT-based emphysema measurement is significantly improved with U-HRCT scans, compared with conventional HRCT scans [13]. Regarding the assessment of the bronchi using U-HRCT scans, some studies have also reported that bronchi with diameters of 1 to 2 mm can be accurately quantified on U-HRCT scans [14, 15]. However, to our best knowledge, there have not been any reports of a detailed analysis of automatic bronchial segmentation of whole lungs on U-HRCT scans that have provided the numbers of bronchi making up each bronchial generation and their total length. The previous observations on U-HRCT scans suggest that compared with conventional HRCT scans, automatic segmentation of U-HRCT scans should provide increased numbers and increased total lengths of peripheral bronchi.

Thus, the aim of study was to evaluate the advantages of U-HRCT scans over conventional HRCT scans for automatic bronchial segmentation performed by a workstation.

Materials and methods

This single-institution retrospective study was approved by our institutional review board. Written informed patient consent was waived.

Patients

This study initially identified 46 consecutive patients who underwent chest CT by a U-HRCT scanner without contrast enhancement as part of routine clinical care in August and September 2018. A total of 13 patients were excluded for the following reasons: previous lung resection ($n=4$), incomplete importation of data from U-HRCT scans ($n=4$), discordance in field of views (FOVs) between U-HRCT and conventional HRCT scans ($n=4$), and excessive bronchiectasis ($n=1$). A total of 33 patients were ultimately enrolled

in the study. Of these, 11 were males and 22 were females. The median age was 66 (range 30 to 80) years. Indications of chest CT were as follows: follow-up for benign lesions ($n=17$), screening for suspected pulmonary nodule ($n=7$), pre-operative evaluation for resectable lung tumor ($n=2$), COPD ($n=2$), interstitial pneumonia ($n=2$), cough ($n=1$), hemoptysis ($n=1$), and rib fracture ($n=1$).

CT scans

All CT scans were performed by a 160-row U-HRCT scanner (Aquilion Precision, Canon Medical Systems, Otawara, Tochigi, Japan). This novel CT scanner is equipped with a 0.25-mm-collimation detector system of 160 detector rows and 1792 channels. CT scans were performed at 120 kVp, 0.25×160 collimation, 0.828 beam pitch, using automatic exposure control. The scanning FOV was individually adjusted from 300 (medium) to 350 (large) mm based on a patient's body habitus. We obtained CT scans from each participant in the supine position, with breath-holding at deep inspiration. Scan data were converted to images by an iterative reconstruction method (AIDR3D ["standard" setting]) and were ultimately reconstructed to 2 different scan series: (1) conventional HRCT mode with 512×512 matrix and 0.5-mm slice thickness and (2) U-HRCT mode with 1024×1024 matrix and 0.25-mm slice thickness. The imaging FOV was fixed at 320 mm, and a reconstruction kernel of FC14 was applied (for the mediastinum).

Image analysis: automatic bronchial segmentation

The image analyses for automatic bronchial segmentation on the U-HRCT and conventional HRCT scans were performed on a research workstation, which was especially designated for U-HRCT scans and which was a modification of a commercially available workstation (Ziostation2, Ziosoft, Tokyo, Japan). For bronchial segmentation, the workstation full automatically extracted bronchial trees (Fig. 1) and determined the total number of bronchi of each generation along with their corresponding total length (third to eighth bronchial generations). This process was performed by a chest radiologist (8 years of experience). If automatic segmentation made obvious mistakes, the course of the corresponding airway's centerline was manually corrected by the radiologist. However, the manual correction did not include expansion of the complete airway tree in the distal direction or indication of the presence of unidentified bronchi.

Image analysis: semiautomatic density measurement of bronchial walls

For the analysis of bronchial wall density, the same chest radiologist used the same research workstation for a manual

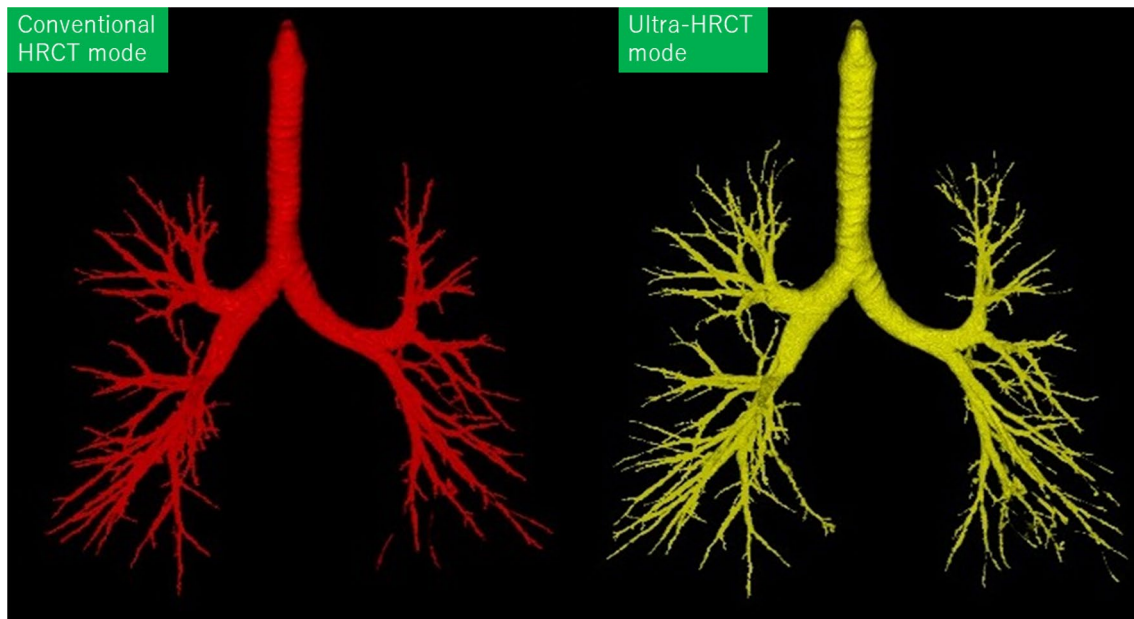


Fig. 1 Comparisons between the U-HRCT and conventional HRCT modes. On the U-HRCT mode (right), several bronchi are automatically segmented by the workstation that are not segmented on the conventional HRCT mode (left)

selection of 3 measured points on the third, fourth, and fifth bronchial generation of each of the 33 patients. The radiologist identified the upper apical segmental bronchus (B1) in the right lung, which was defined as the third generation. After identification of the third-generation bronchus, the fourth and fifth generations were identified on the same bronchial trunk. The sixth- to eighth-generation bronchi were not measured in this analysis, since the identification of the representative points to be measured among the many bronchi in the same generation was difficult. On the images shown by the workstation, the radiologist drew a straight line that overlaid the center of the measured bronchus to create a density curve. For each generation, the density curve was automatically reproduced by the workstation for both the U-HRCT and conventional HRCT modes, since both modes were created from the same raw data. Therefore, the measured points were completely identical for both modes (Fig. 2). We predicted that the curve would include the following density information: lung parenchyma–bronchial wall–air in the bronchial lumen–bronchial wall (on the contralateral side)–lung parenchyma (on the contralateral side) (Fig. 2). The workstation presented the following measures derived from the density curve: the peak wall attenuation (eventually a mean value for the 2 bronchial walls), the bottom (air) attenuation in the bronchial lumen, and bronchial diameter, according to the full-width at half-maximum (FWHM) method. If the peak wall attenuation was higher and the bottom attenuation of the lumen lower, ‘clearer’ bronchial walls were suggested that would result in a larger bronchial diameter.

Statistical analysis

Continuous variables were expressed as mean (standard deviation [SD]). All comparisons between the U-HRCT mode and conventional HRCT mode were performed by the Wilcoxon matched-pair signed-rank test. A *P*-value of < 0.05 was considered significant. All statistical analyses were performed by JMP 15.0 software (SAS Institute, Cary, NC, USA).

Results

Radiation dose

Radiation exposure was assessed according to the volume CT dose index ($CTDI_{vol}$) and the dose–length product (DLP), which were provided by the scanner as information on the dose for each patient. The mean $CTDI_{vol}$ was 7.3 (SD, 1.6) mGy, and mean DLP was 335.3 (SD, 91.4) mGy cm. Both $CTDI_{vol}$ and DLP for U-HRCT were sufficiently lower than the Japanese diagnostic reference level (DRL), in accordance with the Japan Network for Research and Information on Medical Exposures (J-RIME) [16].

Automatic bronchial segmentation: numbers and total lengths of segmented bronchi

The results of the numbers and total lengths of bronchi are shown in Table 1. In the third and fourth bronchial

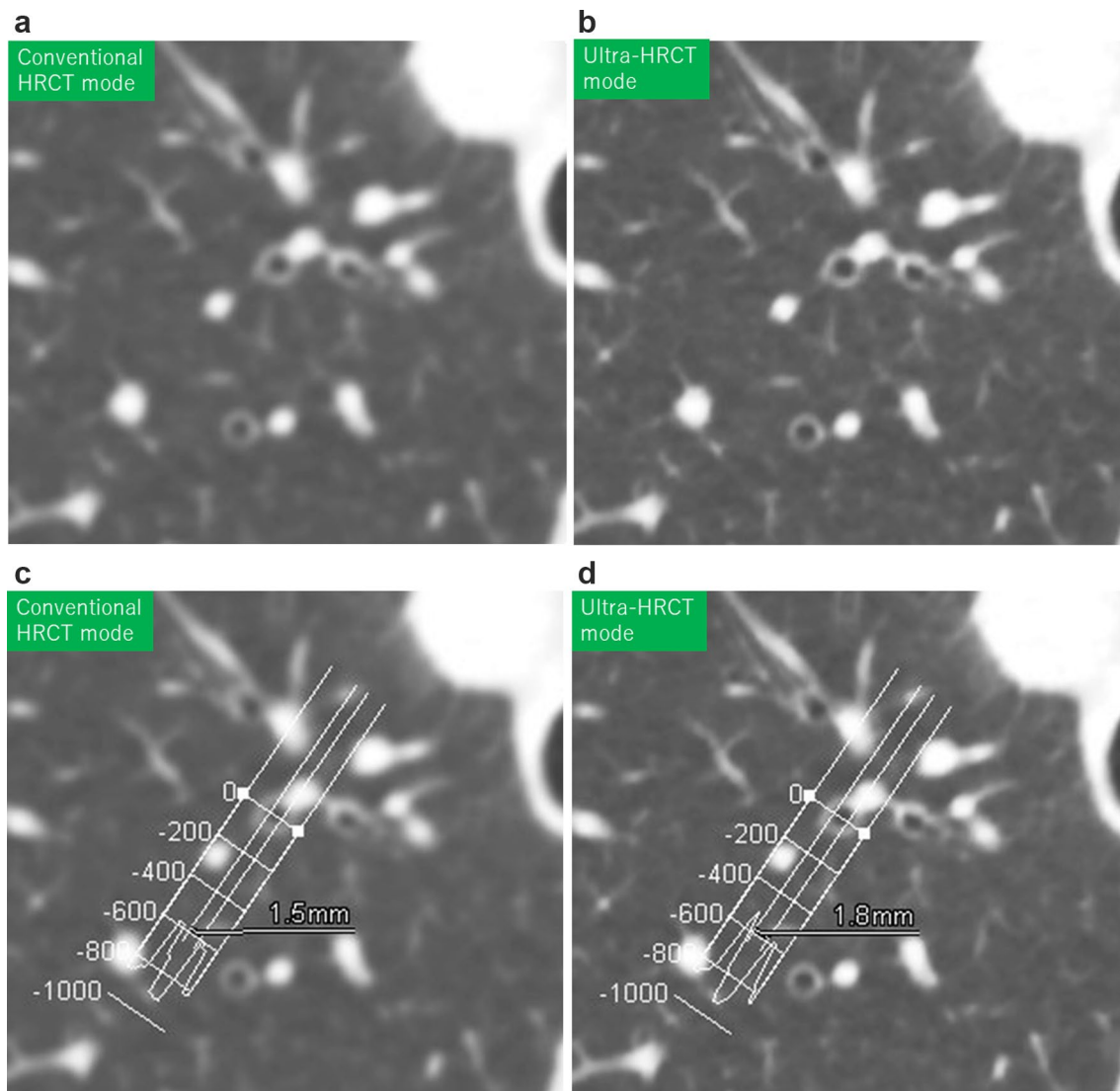


Fig. 2 Example of airway measurement on a density curve. Measurements of a fifth-generation bronchus are demonstrated. On the U-HRCT mode (**b, d**), higher bronchial wall attenuation (-509 and -589 HU) and lower bronchial lumen attenuation (-927 HU) are measured than on the conventional HRCT mode (wall, -583 and

-607 HU; lumen, -910 HU) (**a, c**). The calculated bronchial diameters were 1.8 mm on the U-HRCT mode and 1.5 mm on the conventional HRCT mode. Bronchial walls are more clearly depicted on the U-HRCT mode (**b**) than on the conventional HRCT mode (**a**)

generations, both the U-HRCT mode and the conventional HRCT mode identified almost the same numbers of bronchi. No significant differences were found between the numbers of the third- and fourth-generation segmented bronchi of the 2 modes; however, since small branching points in the proximal bronchi were automatically segmented on the U-HRCT modes, the total lengths of the third- and fourth-generation segmented bronchi were mistakenly longer for the conventional HRCT mode than for the U-HRCT mode for the third-generation bronchi ($P < 0.05$).

By contrast, the U-HRCT mode identified significantly greater numbers of bronchi in the more distal bronchial

generations (from fifth- to eighth-generation bronchi, $P < 0.001$) (Table 1, Fig. 1). While the identified numbers of bronchi increased with each generation (from the third to the sixth generation on the U-HRCT mode), the numbers decreased after the fifth generation on the conventional HRCT mode. Similarly, from the fifth to eighth generations, the U-HRCT mode identified total lengths of the bronchi of each of those generations that were significantly longer than the corresponding total lengths of those generations identified by the conventional HRCT mode ($P < 0.001$).

Table 1 Results of the automatic bronchial segmentation

	Bronchial generation	Mode		P value
		Conventional HRCT [mean (SD)]	U-HRCT [mean (SD)]	
Number of segmented bronchi	Third	18 (1)	18 (1)	0.850
	Fourth	34 (6)	34 (4)	0.864
	Fifth	56 (14)	61 (12)	<0.001
	Sixth	59 (23)	81 (27)	<0.001
	Seventh	36 (23)	71 (36)	<0.001
Total length of segmented bronchi (mm)	Eighth	16 (18)	44 (33)	<0.001
	Third	462 (105)	427 (88)	0.015
	Fourth	857 (233)	867 (193)	0.623
	Fifth	892 (371)	1193 (400)	<0.001
	Sixth	538 (345)	1048 (502)	<0.001
	Seventh	251 (232)	598 (424)	<0.001
	Eighth	90 (148)	287 (335)	<0.001

All values are expressed means (standard deviation). The shorter total length of the 3rd bronchi on the U-HRCT mode than the length on the conventional HRCT mode was due to proximal branching points not identified by the conventional HRCT mode

HRCT high-resolution CT, U-HRCT ultra-HRCT

Analysis of the bronchial density curves

Measurements of the density curves are shown in Table 2. The mean peak wall attenuation decreased as the airways progressed peripherally for both the U-HRCT and conventional HRCT modes. The U-HRCT modes showed significantly higher mean peak wall attenuations, lower bottom lumen attenuations, and wider bronchial diameters for every generation than the conventional HRCT mode ($P < 0.001$) (Fig. 2). These results indicate that the U-HRCT mode successfully and clearly visualized the bronchial wall and

revealed air in the bronchial lumen with sufficiently low CT values (close to the air in the bronchial lumen). The ultimate result was to obtain a wider bronchial lumen than the lumen provided by the conventional HRCT mode.

Discussion

This study found that an automatic airway segmentation technique for the U-HRCT mode with a 1024×1024 matrix and 0.25-mm slice thickness detected peripheral bronchi more accurately than the conventional HRCT mode with a 512×512 matrix and 0.5-mm slice thickness. This result is derived from the higher numbers and longer total lengths of the fifth- to eighth-generation segmented bronchi derived from U-HRCT scans. This advantage of the U-HRCT mode over the conventional HRCT mode could be thought to be derived from the high contrast between the bronchial wall and lumen (air) that is provided by the U-HRCT mode, which is based on our density-curve analysis. The large bronchial diameter and clear bronchial lumen could be easily traced by the workstation for airway segmentation. Altogether, these observations lead us to the recommendation that U-HRCT should be used for several airway analyses, including CT-based bronchial measurements for patients with COPD and virtual bronchoscopy before performing a transbronchial lung biopsy (TBLB).

Automatic airway segmentation has been widely available on several commercial workstations that use software for several different purposes. Automatic bronchial analysis, which is used for thickening of the bronchial wall and narrowing of the bronchial lumen, is also based on automatic airway segmentation. In addition, automatic airway segmentation is important for segmenting the lungs; if the workstation or software cannot segment the entire airway

Table 2 Results of bronchial analysis of a density curve

	Bronchial generation	Mode		P value
		Conventional HRCT [mean (SD)]	U-HRCT [mean (SD)]	
Peak bronchial wall attenuation (HU)	Third	- 294 (169)	- 251 (162)	<0.001
	Fourth	- 548 (137)	- 508 (126)	<0.001
	Fifth	- 669 (133)	- 646 (131)	<0.001
Bottom airway lumen attenuation (HU)	Third	- 1006 (22)	- 1013 (23)	<0.001
	Fourth	- 989 (31)	- 996 (30)	<0.001
	Fifth	- 962 (56)	- 979 (47)	<0.001
Bronchial diameter (mm)	Third	4.4 (1.1)	4.6 (1.1)	0.001
	Fourth	2.8 (0.8)	3.1 (0.8)	<0.001
	Fifth	2.1 (0.8)	2.2 (0.7)	0.004

All values are expressed means (standard deviation). Bronchial diameter was calculated by the full-width at half-maximum method

HRCT high-resolution CT, U-HRCT ultra-HRCT, HU Hounsfield Unit

from the trachea to peripheral bronchi, ‘unsegmented’ airways are involved in the lungs and incorrectly identified as pulmonary emphysema or another cystic pulmonary condition by automatic quantitative analysis performed by the workstation or software. From this viewpoint, the creation of a reliable airway segmentation system provided by a novel technique is important. Although a few reports have illustrated the advantages of U-HRCT for bronchial measurements [14, 15], to the best of our knowledge, this is the first investigation that demonstrates the advantages of U-HRCT for automatic airway (bronchial) segmentation of the entire lung, including the number and total length of the bronchi detected at each generation.

Pathological changes in the structure of the airways, or airway remodeling, produces airflow limitation in obstructive lung diseases such as asthma and COPD. In COPD, chronic inflammatory signals induce epithelial metaplasia, thickening of the smooth muscle layer, fibrosis of the walls of the airways, and degeneration of bronchial cartilage. The result is thickening of the walls of the airways and luminal narrowing [17, 18]. The increased thickness of airway wall as a result of airway remodeling has been investigated as a radiographic marker of disease severity. Various CT-based airway indices have been investigated, including luminal area, percentage of airway wall area, and peak wall attenuation [1–3, 19]. Chest U-HRCT has already been reported to obtain high-quality images, particularly for small bronchi with diameters < 2 mm [6–8, 13–15]. Since conventional HRCT scans provide CT airway indices from more peripheral bronchi (typically fifth-generation bronchi) that are more highly correlated with spirometric values than the CT indices of more proximal bronchi [1–3], our observations could lead to advanced, stabilized quantitative measurements of peripheral bronchi such as sixth- or seventh-generation bronchi for future CT-based COPD studies.

Another clinical application of U-HRCT in chest imaging would be virtual bronchoscopic navigation (VBN) for TBLBs of peripheral pulmonary lesions (PPLs). Virtual bronchoscopy uses volumetric HRCT data to create 3-dimensional images of tracheal and bronchial lumens, which resemble the airways seen on bronchoscopy [20–22]. In VBN, a bronchoscope is guided by virtual bronchoscopy images along a bronchial route to the PPL of interest [23]. In theory, the more accurate bronchial trees provided by U-HRCT should provide more options on the bronchoscopic routes to PPLs and more useful prebronchoscopic navigation. Our data suggest that U-HRCT would be more reliable for VBN before TBLB than conventional HRCT, since U-HRCT can detect the bronchi and bronchial branching points that cannot be visualized by conventional HRCT.

Precise visualization of bronchiectasis in primary lung cancers, particularly in early adenocarcinoma, may

be another clinical application of U-HRCT scans. It has been reported that the presence of bronchiectasis (or intra-tumoral air bronchogram) in ground-glass nodules (GGN) on HRCT scans often suggests malignant components, which can be used for distinguishing atypical adenomatous hyperplasia and adenocarcinomas [24, 25]. If U-HRCT scans can provide more detailed information on bronchiectasis in GGNs than conventional HRCT scans, the U-HRCT scans would be recommended for observing or following up GGNs in daily clinical care.

This study has limitations. First, the ‘conventional HRCT mode’ was created from the raw data obtained by the U-HRCT scanner. That raw data was also used to create the U-HRCT mode. Since the U-HRCT scanner was equipped with an advanced detector system, it can be predicted that the image quality of the ‘conventional HRCT mode’ of this study would be better than the image quality obtained by actual conventional HRCT scanners. However, to avoid unnecessary radiation exposure and guarantee perfect matching between two different (U-HRCT and HRCT) image modes, we believe that reconstruction of the images from the U-HRCT and conventional HRCT modes derived from the same raw data was reasonable. Second, a relatively small number of patients were analyzed. Although we believe that our observations should be similar even if a different patient group were analyzed, unexpected technical limitations might be found for certain patients, such as those with extreme obesity or airway deformation associated with disease. Third, automatic segmentation by novel software might not be perfect, since a minimum manual correction was added. Fourth, since this study enrolled consecutive patients within a short time period, patient backgrounds and reasons for chest CT were diverse. Validation by histopathological findings would be ideal before the application of U-HRCT scans to COPD or other bronchial diseases. Fifth, we did not evaluate the difference in the improvement of bronchial segmentation among the enrolled patients. Since we enrolled patients with different backgrounds, the effect of the U-HRCT mode on bronchial segmentation would have varied. This should be examined by future researches.

In conclusion, CT data reconstructed by the U-HRCT mode with a 1024×1024 matrix and 0.25-mm slice thickness show peripheral bronchi more accurately than data reconstructed by the conventional HRCT mode with a 512×512 matrix and 0.5-mm slice thickness. This technique can be expanded for use in the clinic and in clinical research, by providing quantitative airway measurements for several obstructive diseases or information for use in virtual bronchoscopy.

Acknowledgements The authors thank the engineers and technologists of Ziosoft for their excellent help in developing the research software.

Funding University of the Ryukyus receives a research grant from Canon Medical Systems and Ziosoft.

References

- Matsuoka S, Kurihara Y, Yagihashi K, Hoshino M, Nakajima Y. Airway dimensions at inspiratory and expiratory multisection CT in chronic obstructive pulmonary disease: correlation with airflow limitation. *Radiology*. 2008;248(3):1042–9.
- Hasegawa M, Nasuhara Y, Onodera Y, Makita H, Nagai K, Fuke S, et al. Airflow limitation and airway dimensions in chronic obstructive pulmonary disease. *Am J Respir Crit Care Med*. 2006;173:1309–15.
- Yamashiro T, Matsuoka S, San Jose Estepar R, Dransfield MT, Diaz A, Reilly JJ, et al. Quantitative assessment of bronchial wall attenuation on thin-section CT: an indicator of airflow limitation in chronic obstructive pulmonary disease. *Am J Roentgenol*. 2010;195(2):363–9.
- Hogg JC, Macklem PT, Thurlbeck WM. Site and nature of airway obstruction in chronic obstructive lung disease. *N Engl J Med*. 1968;278:1355–60.
- Kakinuma R, Moriyama N, Muramatsu Y, Gomi S, Suzuki M, Nagasawa H, et al. Ultra-high-resolution computed tomography of the lung: image quality of a prototype scanner. *PLoS ONE*. 2015;10(9):e0137165.
- Yanagawa M, Hata A, Honda O, Kikuchi N, Miyata T, Uranishi A, et al. Subjective and objective comparisons of image quality between ultra-high-resolution CT and conventional area detector CT in phantoms and cadaveric human lungs. *Eur Radiol*. 2018;28(12):5060–8.
- Hata A, Yanagawa M, Honda O, Kikuchi N, Miyata T, Tsukagoshi S, et al. Effect of matrix size on the image quality of ultra-high-resolution CT of the lung: comparison of 512×512 , 1024×1024 , and 2048×2048 . *Acad Radiol*. 2018;25(7):869–76.
- Honda O, Yanagawa M, Hata A, Kikuchi N, Miyata T, Tsukagoshi S, et al. Influence of gantry rotation time and scan mode on image quality in ultra-high-resolution CT system. *Eur J Radiol*. 2018;103(1):71–5.
- Yoshioka K, Tanaka R, Takagi H, Ueyama Y, Kikuchi K, Chiba T, et al. Ultra-high-resolution CT angiography of the artery of Adamkiewicz: a feasibility study. *Neuroradiology*. 2018;60(1):109–15.
- Takagi H, Tanaka R, Nagata K, Ninomiya R, Arakita K, Schuijff JD, et al. Diagnostic performance of coronary CT angiography with ultra-high-resolution CT: comparison with invasive coronary angiography. *Eur J Radiol*. 2018;101:30–7.
- Tanaka R, Yoshioka K, Takagi H, Schuijff JD, Arakita K. Novel developments in non-invasive imaging of peripheral arterial disease with CT: experience with state-of-the-art, ultra-high-resolution CT and subtraction imaging. *Clin Radiol*. 2019;74(1):51–8.
- Nagata H, Murayama K, Suzuki S, Watanabe A, Hayakawa M, Saito Y, et al. Initial clinical experience of a prototype ultra-high-resolution CT for assessment of small intracranial arteries. *Jpn J Radiol*. 2019;37(4):283–91.
- Xu Y, Yamashiro T, Moriya H, Muramatsu S, Murayama S. Quantitative emphysema measurement on ultra-high-resolution CT scans. *Int J Chron Obstruct Pulmon Dis*. 2019;14(1):2283–90.
- Tanabe N, Oguma T, Sato S, Kubo T, Kozawa S, Shima H, et al. Quantitative measurement of airway dimensions using ultra-high resolution computed tomography. *Respir Investig*. 2018;56(6):489–96.
- Tanabe N, Shima H, Sato S, Oguma T, Kubo T, Kozawa S, et al. Direct evaluation of peripheral airways using ultra-high-resolution CT in chronic obstructive pulmonary disease. *Eur J Radiol*. 2019;120:108687.
- Matsunaga Y, Chida K, Kondo Y, Kobayashi K, Kobayashi M, Minami K, et al. Diagnostic reference levels and achievable doses for common computed tomography examinations: results from the Japanese nationwide dose survey. *Br J Radiol*. 2019;92(1094):20180290.
- Higham A, Quinn AM, Cañado JED, Singh D. The pathology of small airways disease in COPD: historical aspects and future directions. *Respir Res*. 2019;20(1):49.
- James AL, Wenzel S. Clinical relevance of airway remodelling in airway diseases. *Eur Respir J*. 2007;30(1):134–55.
- Washko GR, Dransfield MT, Estépar RS, Diaz A, Matsuoka S, Yamashiro T, et al. Airway wall attenuation: a biomarker of airway disease in subjects with COPD. *J Appl Physiol*. 2009;107(1):185–91.
- Horton KM, Horton MR, Fishman EK. Advanced visualization of airways with 64-MDCT: 3D mapping and virtual bronchoscopy. *AJR Am J Roentgenol*. 2007;189(6):1387–96.
- Higgins WE, Ramaswamy K, Swift RD, McLennan G, Hoffman EA. Virtual bronchoscopy for three-dimensional pulmonary image assessment: state of the art and future needs. *Radiographics*. 1998;18(3):761–78.
- Vining DJ, Liu K, Choplin RH, Haponik EF. Virtual bronchoscopy. Relationships of virtual reality endobronchial simulations to actual bronchoscopic findings. *Chest*. 1996;109:549–53.
- Asano F, Eberhardt R, Herth FJ. Virtual bronchoscopic navigation for peripheral pulmonary lesions. *Respiration*. 2014;88(5):430–40.
- Lee HY, Lee KS. Ground-glass opacity nodules: histopathology, imaging evaluation, and clinical implications. *J Thorac Imaging*. 2011;26(2):106–18.
- Oda S, Awai K, Liu D, Nakaura T, Yanaga Y, Nomori H, et al. Ground-glass opacities on thin-section helical CT: differentiation between bronchioloalveolar carcinoma and atypical adenomatous hyperplasia. *Am J Roentgenol*. 2008;190(5):1363–8.

Publisher's Note Springer Nature remains neutral with regard to jurisdictional claims in published maps and institutional affiliations.